1   **SUPPLEMENTARY INFORMATION**

2

3

4   **Bioturbation as a key driver behind the dominance of Bacteria over Archaea**

5   **in near-surface sediment**

6

7

8   **Authors:** Xihan Chen [1], Thorbjørn Joest Andersen [2], Yuki Morono[3], Fumio Inagaki[3], Bo

9   Barker Jørgensen [1], Mark Alexander Lever* [1,4]

10

11   **Author affiliation:**

12   [1] Center for Geomicrobiology, Department of Bioscience, Aarhus University, 8000 Aarhus, Denmark

13   [2] Department of Geosciences and Natural Resource Management, University of Copenhagen, 1350

14   Copenhagen, Denmark

15   [3] Kochi Institute for Core Sample Research, Japan Agency for Marine-Earth Science and Technology

16   (JAMSTEC), Nankoku, Kochi 783-8502, Japan

17   [4] Institute for Biogeochemistry and Pollutant Dynamics, Department of Environmental Systems

18   Sciences, ETH Zürich, 8092 Zürich, Switzerland

19

20   **Correspondence:** mark.lever@usys.ethz.ch

21

24   **Supplementary Results**

25   **Method comparisons**

26   Our interpretations of archaeal and bacterial 16S gene abundance profiles assume that the

27   DNA extraction and 16S gene amplification data reflect real trends within sediments rather

28   than biases introduced by the DNA extraction method or primer choices. Using M1 sediment,

29   we had previously shown good comparability in overall trends of archaeal and bacterial 16S

30   gene abundances between our extraction method and a commercial DNA extraction kit

31   (reference #6, Fig. 10c,d). We here additionally performed epifluorescence microscopic cell

32   counts at M22A, M27A, M29A, M1, and M5 (Supplementary Fig. 7) and calculated gene

33   copy numbers per cell by dividing the sum of archaeal and bacterial 16S gene abundances per

34   sample by cell abundance data from the nearest sample in which cell numbers were

35   quantified. These calculations enabled us to check whether calculated average gene copies

36   per cell were in a realistic range. Published global mean±standard deviations of 16S gene

37   copies per cell are 4.12±2.75 for Bacteria and 1.61±0.88 for Archaea

38   (https://rrndb.umms.med.umich.edu/). Average values of 1-7 16S gene copies per cell would

39   thus indicate good agreement between qPCR and cell count data. By contrast, values >7 16S

40   gene copies per cell would suggest poor agreement, e.g. due to inclusion of high numbers of

41   16S genes from outside of living cells or poor cell extraction and cell enumeration efficiency.

42   Similarly, values of <1 16S gene copies per cell would indicate poor agreement, e.g. caused

43   by low extraction efficiency of the DNA extraction method.

44   The cell abundance profiles match a previously proposed cell distribution model for

45   marine sediments[29] (Supplementary Fig. 8a). Calculated 16S gene copies per cell mostly

46   range between 1 and 5, suggesting a good match between 16S gene abundances and cell

47   counts (Supplementary Fig. 8b; site averages±standard deviation: M22A: 4.3±4.2; M27:

48   2.2±1.4; M29A: 4.2±2.5; M5: 2.0±1.4 copies cell^{-1}). This good agreement is remarkable

49   given that cell and 16S gene abundances were quantified using independent extraction and

50   quantification methods, and that DNA was extracted from different sediment aliquots and

51   slightly different sediment depths than cells for cell counts. Noteworthy is also the absence of

52   a clear, depth-related change in calculated 16S genes per cell, in spite of the shift from

53   bacterial dominance in the bioturbation zone to similar population sizes of Bacteria and

54   Archaea in deeper layers. This suggests that Bacteria and Archaea have similar numbers of

55   16S genes per cell in surface and subsurface marine sediments of Aarhus Bay (also see

56   Discussion).

57   We furthermore investigated the possibility that our domain-specific qPCR primer

58   pairs introduced strong biases, which led to the observed trends in archaeal and bacterial

59   distributions (info on primer combinations in Supplementary Methods). Indeed, while

60   agreement was good in bioturbated surface sediments, we observed significant, primer-

61   dependent differences in archaeal 16S gene abundance estimates in subsurface sediments,

62   with our archaeal primer choice resulting in higher estimates than two other archaeal primer

63   combinations (Supplementary Fig. 6a). By contrast, bacterial 16S gene abundances estimated

64   using three different bacterial primer pairs showed a better agreement (Supplementary Fig.

65   6b). Despite these primer-related differences, the overwhelming dominance of bacterial over

66   archaeal 16S genes in surface sediments, and the comparable 16S gene abundances of the two

67   domains in subsurface sediments were confirmed (Supplementary Fig. 6c).

68

69

70   **Supplementary Methods**

71   **Additional Primer Checks**

72   We performed additional qPCR assays to compare gene copy numbers obtained with three

73   different archaeal and three different bacterial qPCR primer combinations on five sediment

74 depths from station M1 (5, 80, 160, 310 and 1055 cmbsf). At each sediment depth we

75 performed three replicate DNA extractions. In addition, we ran three replicate qPCR assays

76 on each individual extract. The three archaeal primer pairs used were: (1) Arc806F-Arc958R

77 (described in the Methods), (2) Arc806F-Arc915Rmod (5'-GTG CTC CCC CGC CAA TT-

78 3')[3], and (3) Arc915Fmod (5'-AAT TGG CGG GGG AGC AC -3')[3] - Arc1059R (5'-GCC

79 ATG CAC CWC CTC T-3')[4]. The three bacterial primer pairs were: (1) Bac8Fmod-

80 Bac338Rabc (described in the Methods), (2) Bac806F_mod2 (5'-AAC RGG ATT AGA TAC

81 CCT GGT AGT CC-3')[5] - Bac908R_mod (5'- CCC GTC AAT TCM TTT GAG TT-3')[6], and

82 (3) Bac908F_mod (5'-AAC TCA AAK GAA TTG ACG GG-3')[6] - Bac1075R (5'-CAC GAG

83 CTG ACG ACA RCC-3')[7]. The thermal cycler protocols were the same as described in the

84 Methods, except that an annealing temperature of 56°C was used for all bacterial assays, and

85 an elongation time of 15s was used for all archaeal assays.

86

Core descriptions (2012)

88 Ten Rumohr cores were taken each from M1 and from M5 in March 2012 and described

89 based on sediment color changes and distributions of burrows. All of these cores showed

90 visual signs of an oxidized surface mixed layer (SML), where sediments had a predominantly

91 light brown color. This layer was typically 4±1 cm thick. Below this SML, sediments became

92 predominantly dark grey, presumably due to the accumulation of iron(II) sulfides, while

93 locally still containing light brown streaks, that indicated occasional transport of oxidized

94 surface sediments to deeper layers by macrofauna. This deep mixed layer (DML) extended

95 from approximately 4 to 10 cmbsf at station M1. At M5, the DML was more variable in

96 depth, ranging from ~4-12 cm in the microbiology core, and from ~4 to 7 to ~4 to 20 cmbsf

97 in the other nine cores. All Rumohr cores had worm burrows. These burrows ranged down to

98 22 cmbsf and 17 cmbsf in the microbiology cores from M1 and M5, respectively. In the other

99   cores, the burrows ranged down to 15 to 27 cmbsf at M1, and to 14 to 40 cmbsf at M5. Deep-

100   ranging burrows were typically ~1 cm in diameter, ranged in direction from sloping to nearly

101   horizontal, and had rough-textured inner walls with no lining and no signs of oxidation.

102   Macrofauna were observed in two cores: one worm (*Heteromastus filiformis*) was present at

103   10 cm sediment depth in the core from M1; this core was also used for methane, DIC, and

104   TOC analyses. Furthermore, one small specimen of *Echinocardium cordatum* (diameter ~0.5

105   cm) was found in surface sediment of the microbiology core from M5. Below the DML,

106   sediments remained dark grey until a second color change, from dark grey back to a lighter

107   brown, occurred further below. The depth of this color transition was highly variable,

108   occurring between 28-48 cmbsf at M1, and between 35-57 cmbsf at M5, and correlates with a

109   strong decrease in microbial sulfate reduction rates between 30 and 50 cmbsf at M1[1, 2], and

110   roughly with the depth of the SMTZ at M5. This deep color transition could be due to

111   decreased sulfate reduction rates and consequentially lower accumulation of iron(II) sulfides

112   in layers below the transition.

113   The sediment cores from Aarhus Harbor differed markedly from the Aarhus Bay

114   stations in that macrofauna or any signs of macrofaunal activity were absent. Sediments were

115   uniformly black below the top ~1 mm, presumably due to high rates of sulfate reduction and

116   metal sulfide precipitation.

117

118   **Archaeal and bacterial community compositions at M1**

119   The same DNA extracts from five depths at M1 and the same archaeal and bacteria primer

120   pairs as described above were used for PCR followed by DNA sequencing. Each 50-µL PCR

121   reaction mixture (1st PCR) contained 25 µl 2× KAPA HiFi HotStart ReadyMix (Kapa

122   Biosystems), 0.4 µM of each primer, and 1 µL DNA template. The thermal cycler protocols

123   were (1) enzyme activation and initial denaturation at 95°C for 5 min; (2) 15 cycles of (a)

124 denaturation at 98°C for 20 sec, (b) primer annealing at 56°C (A1 and A2) and 60°C (A3, B1,

125 B2 and B3) for 30 sec, and (c) elongation at 72°C for 15 sec; (3) final extension at 72°C for 5

126 min. PCR products were visualized using gel electrophoresis and cleaned using the

127 Agencourt Ampure XP kit (Beckman Coulter, Brea CA). Cleaned PCR products were

128 subjected to a second PCR amplification with barcoded PCR primers (8 bp barcode) in

129 preparation for multiplex amplicon sequencing on an Ion Personal Genome Machine (PGM™)

130 system (Ion Torrent, Life Technologies). PCR protocols with barcode-tagged primers were

131 the same as for the first PCR, except that the 1st PCR product was used as a DNA template,

132 the annealing temperature was 5°C higher, and 27 thermal cycles were used. The barcoded

133 PCR products were visualized using gel electrophoresis and cleaned using the Agencourt

134 Ampure XP kit as for the 1st PCR products. Cleaned PCR products were quantified using the

135 Qubit hs-DS-DNA kit (Invitrogen) on a Qubit® 2.0 Fluorometer (Invitrogen, Life

136 Technologies) reading at 485 nm excitation and 530 nm emission, pooled at equimolar

137 concentrations of each barcoded PCR product, and sequenced using an Ion PGM™ system

138 with one 314 chip and one 316 chip.

139   Sequence de-multiplexing and bioinformatic processing were performed using Mothur

140 pipelines[8]. Sequences were analyzed individually for each primer pair, since the amplicons

141 covered different regions. Initial quality filtering excluded all sequences that were shorter

142 than 100 bp or contained primer mismatches, homopolymer runs >8 bp, or a mean quality

143 score below 20. Acacia was used to correct amplicon pyrosequencing errors[9]. Uchime was

144 used to detect chimeric sequences[10], which were removed before OTU classification. The

145 high quality sequences were then clustered using an average neighbor algorithm at a 97%

146 sequence similarity cutoff. OTUs with singleton reads were filtered and dropped before

147 further analysis. OTUs were given taxonomic assignments based on full-length sequences

148 and taxonomy references from Silva Release 119

149   (http://www.mothur.org/wiki/Silva_reference_files). For each primer pair, the libraries

150   generated for each of the three DNA extracts per sediment depth were used to calculate

151   average percentages of each taxonomic group, which were then used in all analyses on

152   archaeal and bacterial community structure.

153   To compare the community compositions across the different primer pairs and depths

154   analyzed, pairwise sample similarities (Bray Curtis) of archaeal and bacterial sequences were

155   calculated at the species level and visualized using Unweighted Pair Group Method with

156   Arithmetic Mean (UPGMA) trees by software PAST[11].

157

Supplementary Tables

Supplementary Table 1: Basic information on sampling stations. mbsf, meters below seafloor; SMTZ = sulfate-methane transition zone, defined as the depth interval where the concentration ratio of sulfate to methane ranges from 2:1 to 1:2, and where the highest rates of anaerobic oxidation of methane occur; N/A = not applicable, because this depth was not reached in the cored interval, ND = not determined.

Station	Location	Water Depth (m)	Sampling Time	Core length (mbsf)	Depth interval of SMTZ (mbsf)	Depth of free CH_4 gas (mbsf)
M21	56°06.810′N, 10°24.714′E	18.4	Oct. 2009	2.97	N/A	N/A
M22A	56°06.745´N, 10°24.880´E	18.8	May 2010	4.82	N/A	N/A
M24	56°06.713′N, 10°24.981′E	18.8	Oct. 2009	5.80	3.36-4.31	N/A
M26	56°06.693′N, 10°25.029′E	19.1	Oct. 2009	5.54	3.04-3.78	7.04
M27A	56°06.679´N, 10°25.083´E	19.1	May 2010	7.12	2.62-2.90	4.70
M29A	56°06.645´N, 10°25.175´E	19.3	May 2010	7.20	2.20-2.75	4.45
M1	56°09.167′N, 10°19.333′E	15.0	Oct. 2009	10.85	1.40-1.60	4.00
			May 2010	9.20	1.94-2.03	ND
			March 2012	0.62	N/A	N/A
M5	56°06.333′N, 10°27.800′E	27.0	May 2010	6.70	0.47-0.58	1.00
			March 2012	0.81	0.48-0.56	N/A
AHB	56°08.324′N, 10°12.877′E	~2.0	July 2012	0.15	N/A	N/A

Supplementary Table 2: Summary of average bacterial and archaeal 16S gene abundances and BARs across 8 stations and 4 biogeochemical zones. Archaeal and bacterial 16S gene copy numbers are shown in units of 10^8 copies cm^{-3} of wet sediment.

Zones / Stations		Bioturbation zone			Sulfate zone			SMTZ			Methane zone		
		mean±std.	range	*n*	mean±std.	range	*n*	mean±std.	range	*n*	mean±std.	range	*n*
M21	Archaea	1.44±0.89	0.21-2.30	*3*	1.82±1.67	0.23-4.57	*4*	0.27	0.06	*2*	/	/	*0*
	Bacteria	19.68±4.73	13.10-24.01		3.23±2.95	0.10-7.73		0.09	0.00		/	/	
	BAR	28.33±24.13	10.42-62.43		1.48±0.70	0.43-2.37		0.33	0.06		/	/	
M22A	Archaea	1.30±0.72	0.58-2.02	*2*	2.12±1.75	0.25-4.95	*5*	0.73	0.73	*1*	/	/	*0*
	Bacteria	18.59±1.43	17.16-20.02		4.32±3.54	0.38-9.86		0.61	0.61		/	/	
	BAR	21.52±13.01	8.52-34.53		1.97±0.33	1.35-2.24		0.84	0.84		/	/	
M24	Archaea	2.30±1.34	0.91-4.10	*3*	1.80±1.30	0.32-3.40	*4*	0.13±0.03	0.10-0.16	*3*	0.16±0.02	0.14-0.18	*2*
	Bacteria	30.87±5.78	24.70-38.61		4.07±3.30	0.58-7.55		0.15±0.02	0.12-0.17		0.11±0.00	0.11-0.12	
	BAR	21.30±15.40	6.02-42.37		2.00±0.54	1.30-2.78		1.16±0.09	1.05-1.25		0.71±0.12	0.59-0.84	
M26	Archaea	0.78±0.21	0.55-1.05	*3*	1.77±1.46	0.40-4.12	*4*	0.63±0.23	0.34-0.91	*3*	0.36±0.10	0.28-0.50	*3*
	Bacteria	35.79±11.70	25.35-52.13		3.47±2.78	0.62-8.05		0.49±0.16	0.28-0.66		0.26±0.08	0.19-0.37	
	BAR	46.17±8.14	34.95-53.99		2.23±1.17	1.20-4.20		0.78±0.04	0.73-0.80		0.71±0.06	0.62-0.78	
M27A	Archaea	2.09±0.96	1.14-3.05	*2*	2.51±1.93	0.13-4.30	*5*	0.41±0.22	0.22-0.72	*3*	0.19±0.04	0.14-0.23	*4*
	Bacteria	26.44±4.81	21.63-31.25		5.52±4.71	0.38-13.00		0.57±0.12	0.45-0.73		0.18±0.10	0.07-0.32	
	BAR	17.30±10.21	7.09-27.50		2.53±0.88	1.66-4.00		1.63±0.53	1.02-2.32		0.86±0.36	0.50-1.43	
M29A	Archaea	3.04±2.09	0.95-5.13	*2*	3.29±2.66	0.10-6.81	*5*	0.59±0.33	0.27-1.05	*3*	0.48±0.24	0.24-0.87	*4*
	Bacteria	36.80±7.59	29.21-44.39		6.40±4.91	0.29-12.31		0.77±0.06	0.71-0.86		0.52±0.17	0.25-0.70	
	BAR	26.24±20.55	5.70-46.79		2.35±0.52	1.81-2.98		1.72±0.80	0.82-2.76		1.22±0.49	0.71-2.02	
M1(2009)	Archaea	0.89±0.13	0.77-1.02	*2*	2.89±0.63	2.04-3.75	*4*	3.11±1.76	1.18-5.43	*3*	1.40±0.21	1.23-1.76	*4*
	Bacteria	43.84±6.85	36.99-50.70		5.11±2.36	5.41-34.43		3.01±1.85	1.39-5.59		1.06±0.27	0.80-1.46	
	BAR	51.17±14.98	36.19-66.15		1.78±0.69	0.94-2.53		0.99±0.18	0.75-1.18		0.78±0.27	0.46-1.19	

Zones / Stations		Bioturbation zone			Sulfate zone			SMTZ			Methane zone		
		mean±std.	range	*n*	mean±std.	range	*n*	mean±std.	range	*n*	mean±std.	range	*n*
M5(2010)	**Archaea**	/	/	*0*	1.25±1.13	0.37-2.84	*3*	1.46±0.12	1.37-1.64	*3*	0.83±0.51	0.24-1.48	*3*
	Bacteria	/	/		3.81±3.71	1.15-9.05		6.01±2.71	3.42-9.75		2.56±1.79	0.42-4.80	
	BAR	/	/		2.85±2.49	2.22-3.19		4.23±5.30	2.09-7.06		2.74±0.71	1.74-3.26	
M1(2012)	**Archaea**	2.72±0.58	1.98-3.64	*7*	3.05±1.12	1.41-5.52	*12*	/	/	*0*	/	/	*0*
	Bacteria	25.22±17.55	6.25-56.81		5.97±2.01	4.01-11.60		/	/		/	/	
	BAR	8.90±6.18	2.65-21.92		2.08±0.56	1.33-2.95		/	/		/	/	
M5(2012)	**Archaea**	2.57±0.77	1.32-3.52	*7*	3.63±1.07	1.95-5.30	*9*	3.41±1.83	1.65-5.93	*3*	3.55±1.22	2.27-5.58	*5*
	Bacteria	18.05±12.00	7.80-44.97		8.00±1.92	4.73-10.44		6.34±3.25	3.08-10.77		4.94±1.35	3.67-6.98	
	BAR	7.81±5.31	2.71-16.39		2.27±0.32	1.76-2.78		1.88±0.06	1.82-1.95		1.43±0.14	1.25-1.63	
Overall	**Archaea**	2.10±1.18	0.21-5.13	*31*	2.65±1.68	0.10-6.81	*55*	1.27±1.51	0.10-5.93	*24*	1.20±1.37	0.14-5.58	*25*
	Bacteria	26.24±13.80	6.25-56.81		5.54±3.50	0.10-13.00		2.20±2.94	0.08-10.77		1.61±2.01	0.07-6.98	
	BAR	20.54±18.97	2.65-66.15		2.15±0.70	0.43-4.20		1.61±1.36	0.28-7.06		1.21±0.72	0.46-3.26	

Supplementary Table 3: List of the dominant sediment macrofauna and their size, burial depth and feeding mode in central Aarhus Bay.

Type	Species	Adult size (cm)	Burial depth	Feeding mode and depth	References
Bivalves	*Abra alba*	2.5	0.5-2.5 cm[*]	Mainly surface deposit feeder, but also suspension feeder	[12, 13]
	Mysella bidendata	0.3	Surface, burrows of other species, crevices	Surface deposit and suspension feeder; mainly deposit feeder in Aarhus Bay	[14-17]
	Corbula gibba	1.5	1-2 cm	Surface suspension feeder	[18, 19]
	Macoma calcarea	3.5-5	0-10 cm	Surface deposit feeder, suspension feeder	[20]
Polychaetes	*Terebellides stroemi*	7.5	Tube extends to several cm below sediment surface	Sedentary surface deposit feeder that builds a tube, preference for small, low-gravity particles	[21]
	Nephtys ciliate, Nephtys sp.	10-30	Commonly to 5-10 cm, but also deeper	Predator, scavenger, deposit feeder; builds temporary burrows; biodiffusor	[22-24]
	Heteromastus filiformis	Length: 10, width: 0.1	0-30 cm	Subsurface deposit feeder with upward conveyor belt transport, builds burrows	[13, 14, 21]
	Pectinaria sp.	4.5	Tubes extend to 5 cm depth	(Mainly subsurface) deposit feeder with upward conveyor belt transport, builds tube	[14, 25]
Echinoderms	*Ophiura albida*	Disc: 1.5, arms: 6	Stays at surface	Surface predator, scavenger, deposit feeder	[15]
	Echinocardium cordatum	5	0-15 cm	Surface deposit feeder, surface to subsurface burrower	[26]

[*]inferred from close relative *Abra nitida*

Supplementary Figures

Supplementary Figure 1: Map of Aarhus Bay, Denmark, with locations of sampling stations (modified from reference #27). The gray shades indicate the shallowest depth at which free gas bubbles appear.
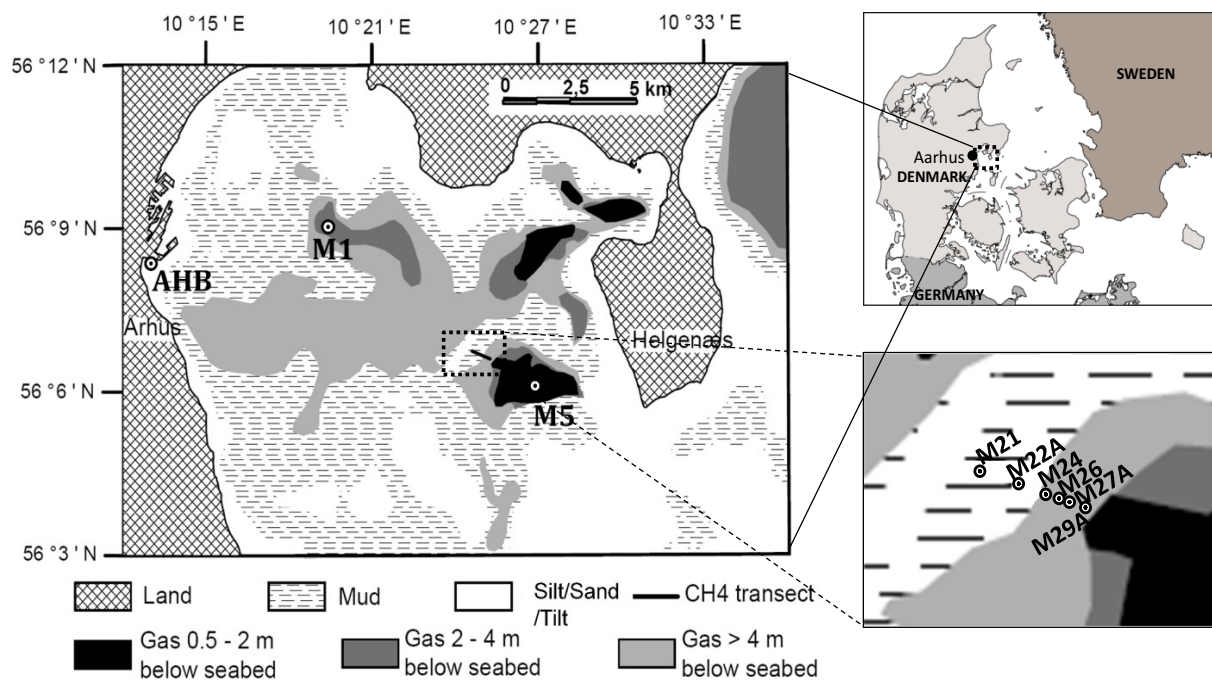
Supplementary Figure 2: Depth distributions of archaeal and bacterial 16S gene abundances across the CH$_4$ transect in Aarhus Bay (M21-M29A), and at Stations M1 and M5. The lower figures show data from the upper figures at high resolution for the top 0.5 m. Grey shaded areas mark the depth interval of the SMTZ (also see Supplementary Table 1). Sediments above belong to the sulfate zone (SZ), sediments below belong to the methane zone (MZ; also see labeling in figure for M24). The gray circle at M21 indicates samples from an organic-poor glacial sand layer at the bottom of M21. The SMTZ and MZ were not reached by coring at M21 and M22A.

Supplementary Figure 2

Archaea & Bacteria (gene copies cm^{-3})
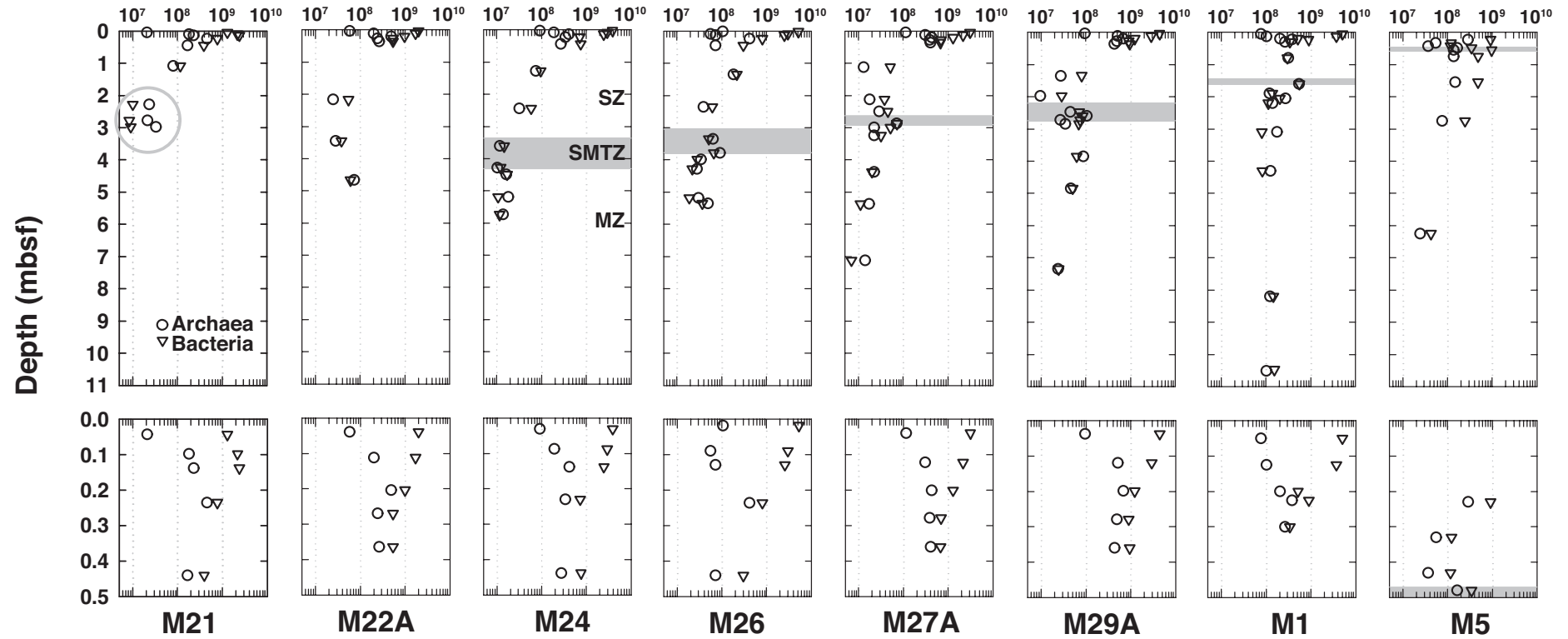
Supplementary Figure 3: Fine-scale geochemical profiles at Stations M1 (top) and M5 (bottom). (a, b) methane concentrations; **(c, d)** total organic carbon (TOC) in weight % (wt%); **(e, f)** porosity; **(g, h)** density. The horizontal grey dashed line spanning all panels marks the depth to which significant sediment reworking was detected (0.14 mbsf). The grey zone at M5 marks the SMTZ. All data were obtained from Rumohr cores collected in March 2012.

Supplementary Figure 3
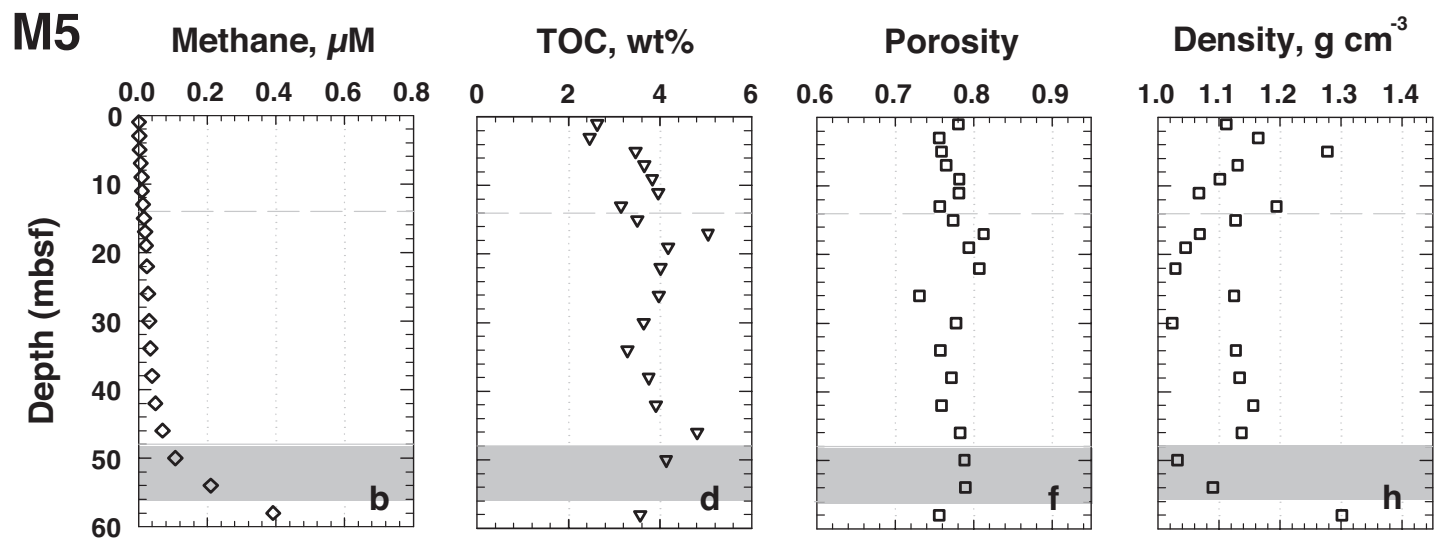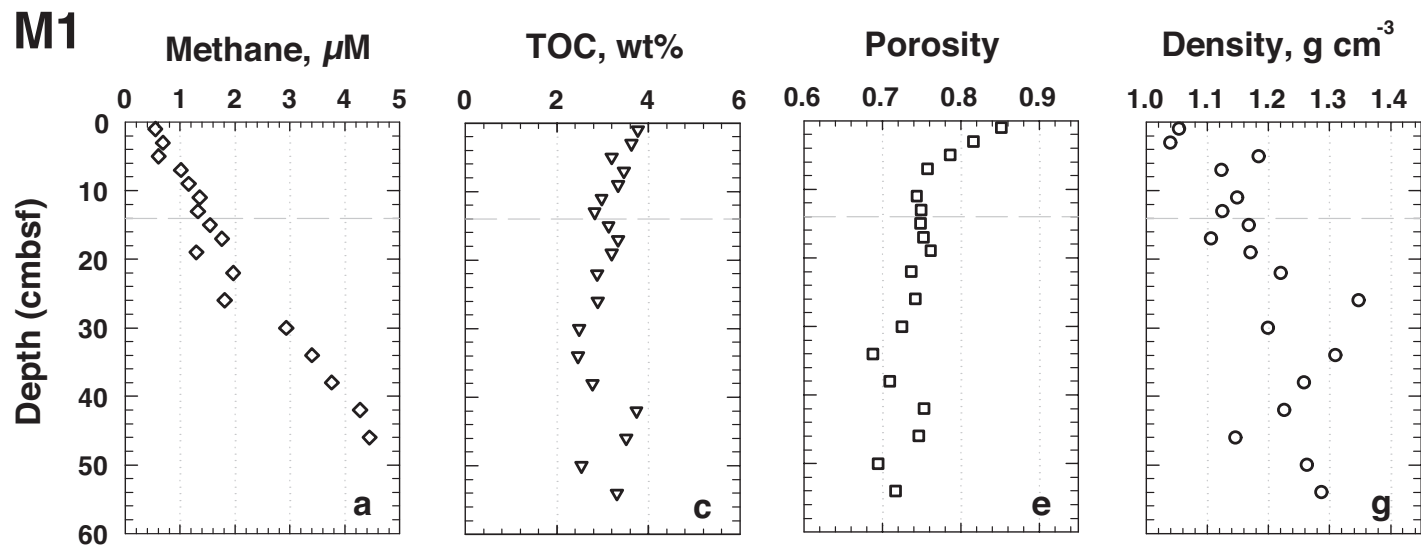
Supplementary Figure 4: (a) Archaeal and bacterial 16S gene abundances, and (b) BARs in surface sediment at the bioturbation-free control site in Aarhus Harbor (AHB) compared to stations in Aarhus Bay.
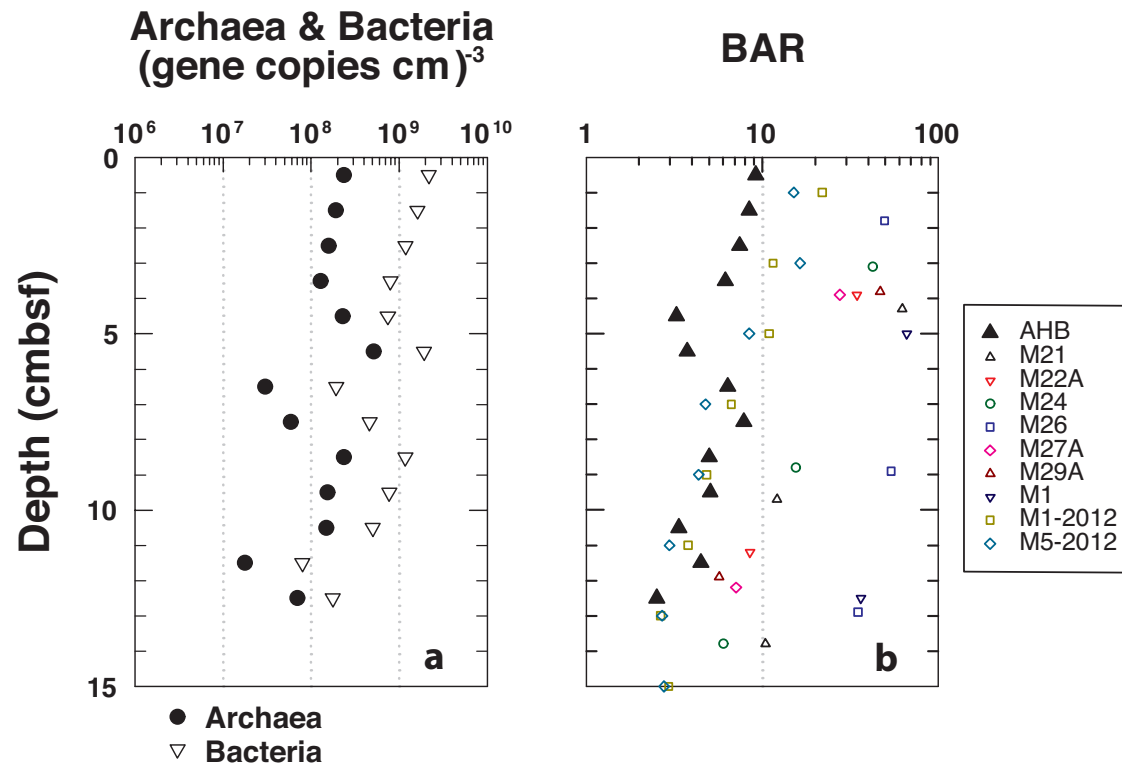
Supplementary Figure 5: Scatter plots illustrating the relationships between TOC, TN, C:N, δ^{13}C-TOC, and δ^{15}N-TN and BAR, archaeal 16S gene abundances, and bacterial 16S gene abundances. (**a**) Samples spanning the bioturbation zone; (**b**) samples spanning sediments underlying the bioturbation zone; (**c**) samples spanning sediments underlying the bioturbation zone excluding all terrestrial samples. R^2-values are for the trendline shown in each plot. Statistical significance of the correlations was determined using a Spearman's Rank Correlation test (ns = not significant; asterisks indicate statistical significance with the number of asterisks indicating the level of significance: * for $p<0.05$, ** for $p<0.01$, and *** for $p<0.001$).

Supplementary Fig 5a

|	TOC	TN	C:N	δ¹³C-TOC	δ¹⁵N-TN
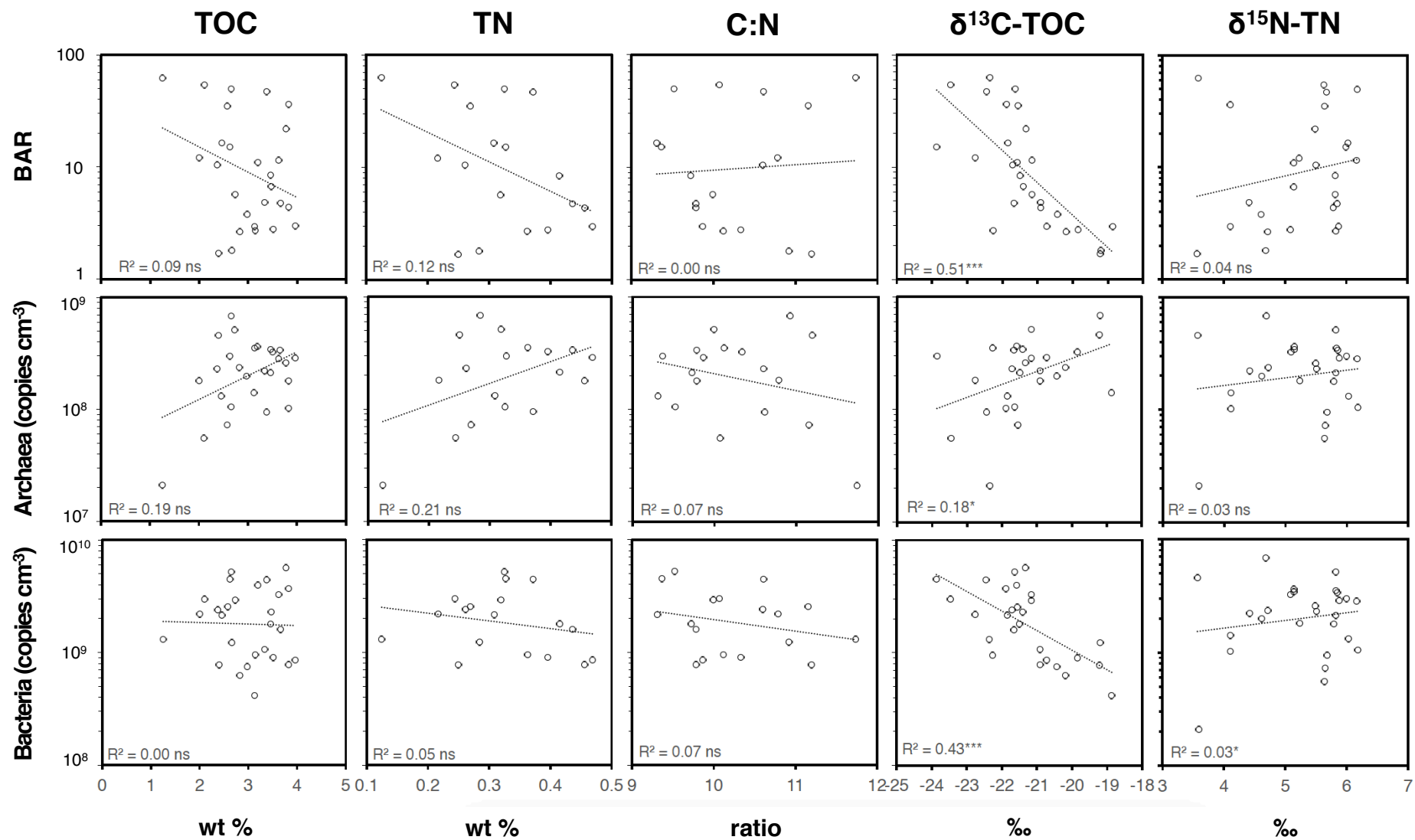
Supplementary Fig. 5b
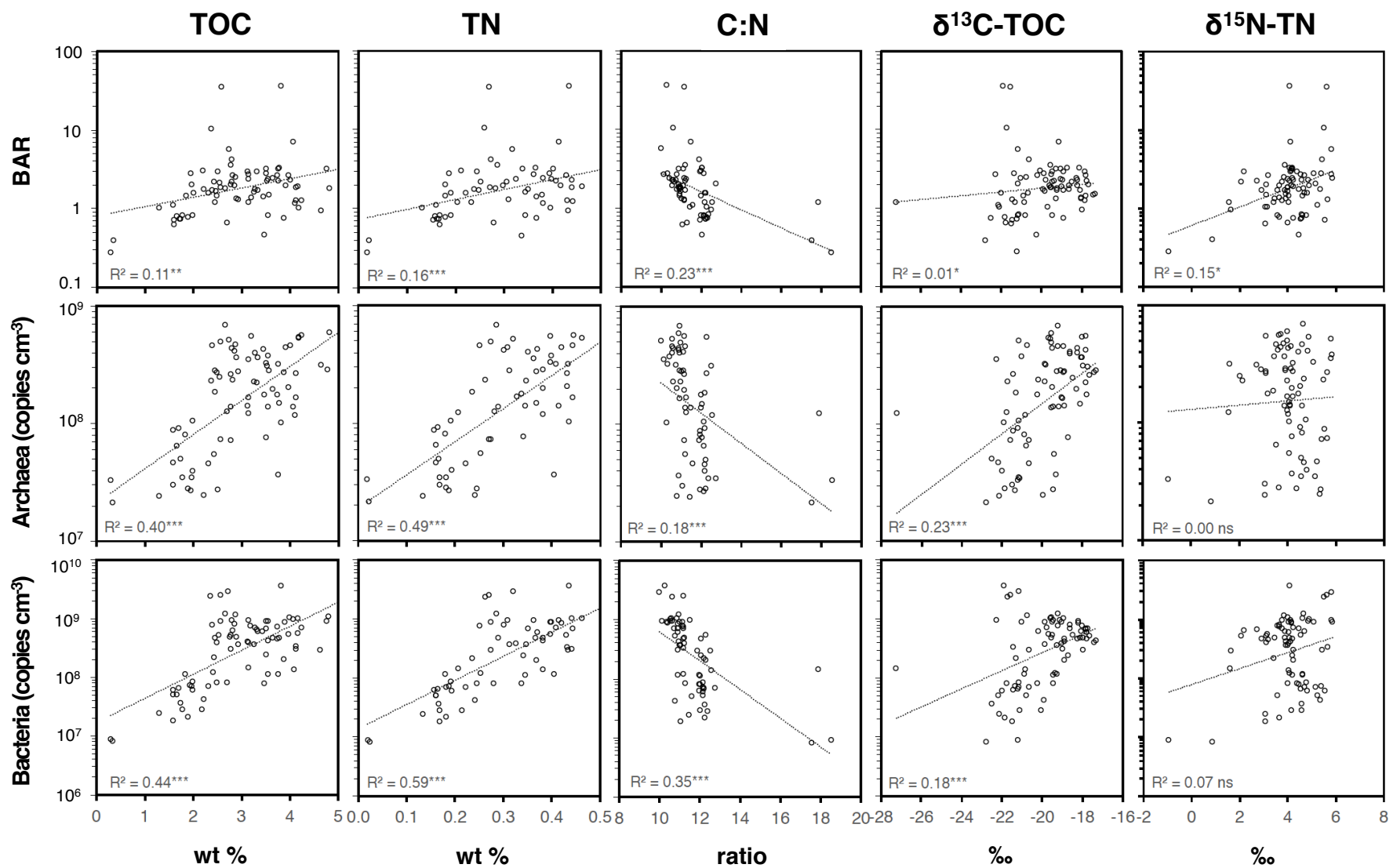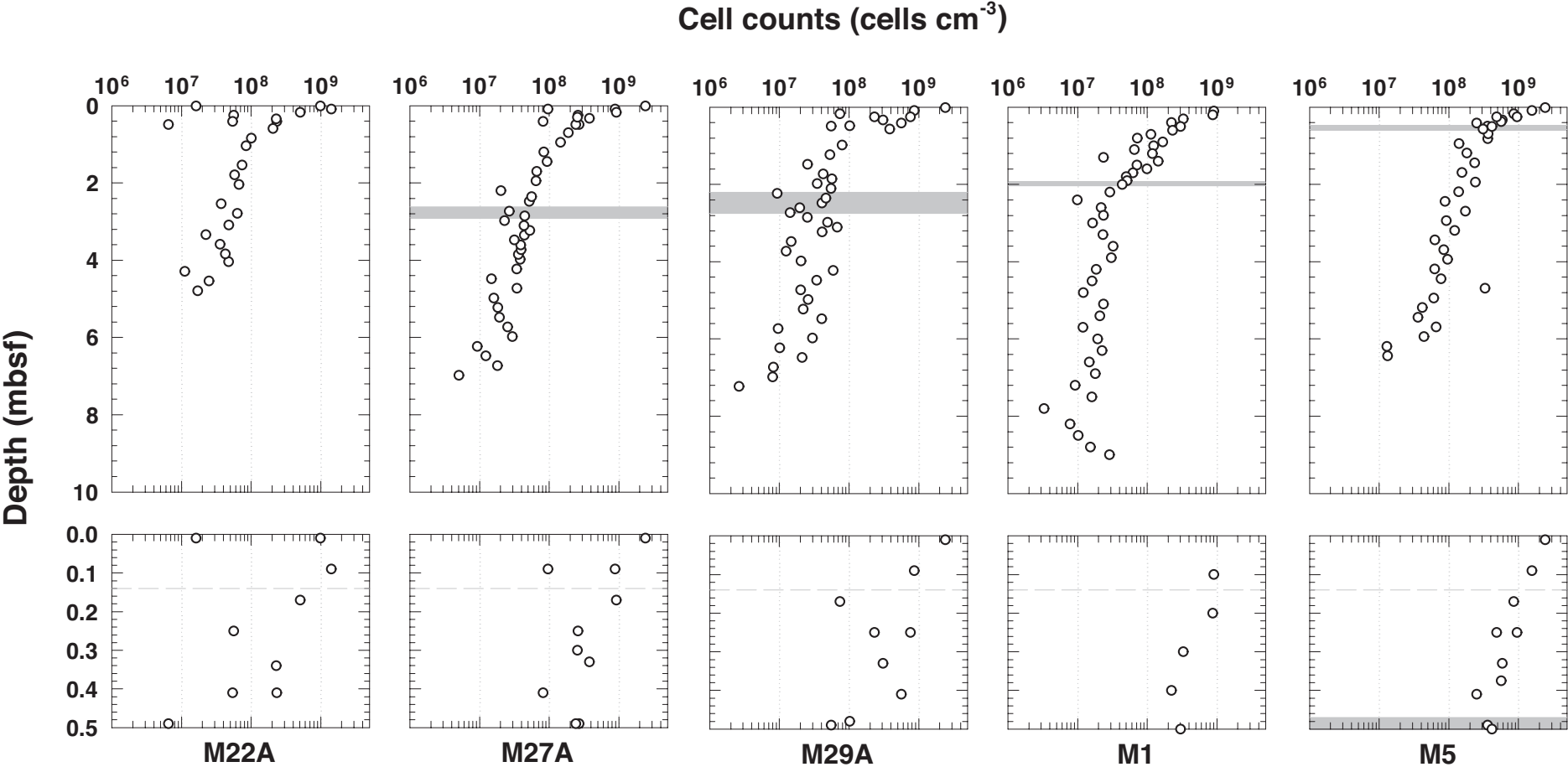
Supplementary Fig. 5c
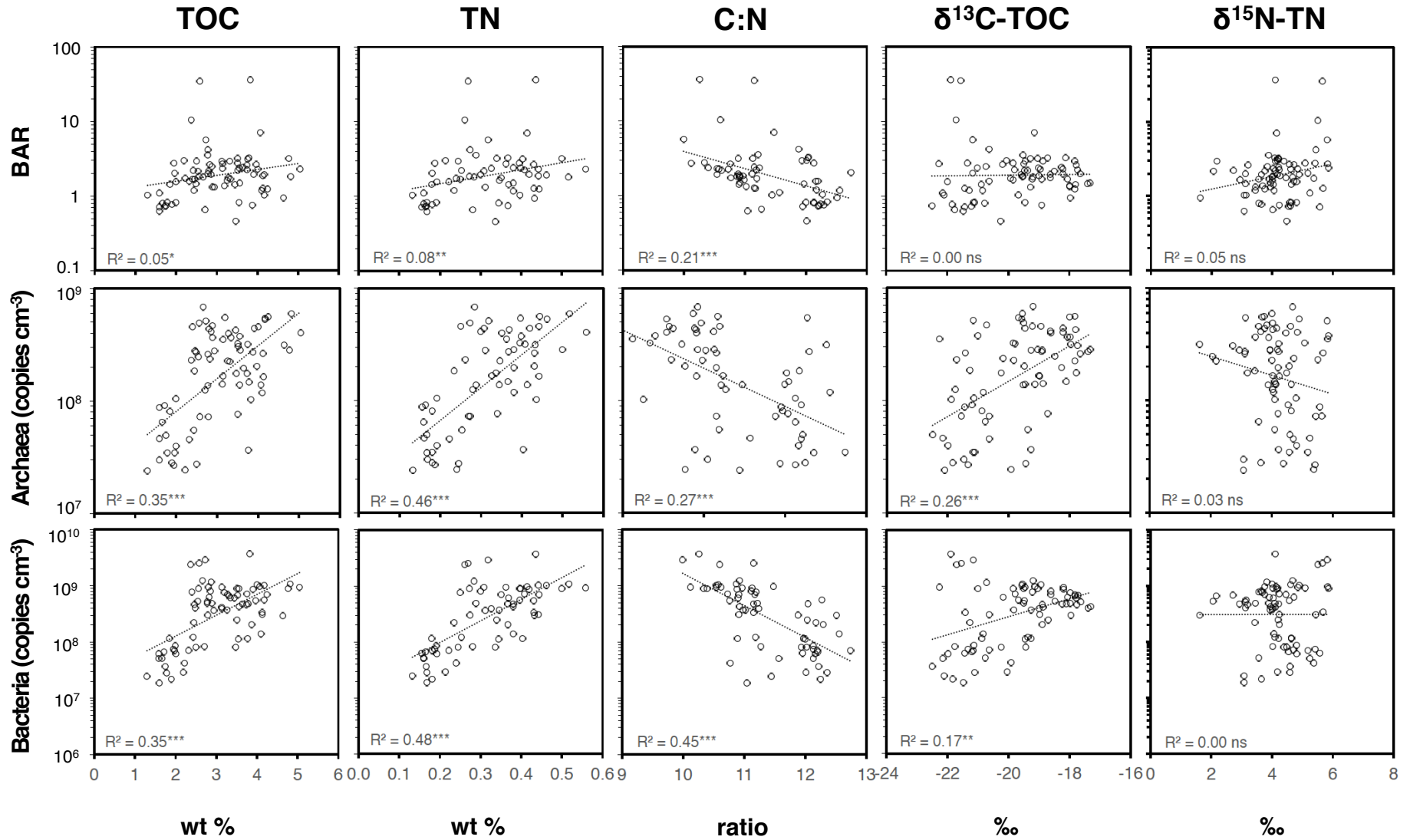
Supplementary Figure 6: (a) Archaeal and (b) bacterial 16S gene abundances yielded by different primer pairs on three extraction replicates per depth at M1; (c) box plots of BARs. (a, b) Three qPCR replicates were applied on each of the three extraction replicates and primer combinations. The average values for each extraction replicate and primer combination are plotted. (c) Box plots were based on BARs calculated from each of the bacterial and archaeal primer pair combinations (3 archaeal × 3 bacterial primer pairs, thus n=9). Blue lines inside boxes indicate average values, black lines indicate median values. Boxes indicate 25% and 75% confidence intervals. Error bars indicate 10 and 90% confidence intervals. The primer combinations Arc 806F-Arc 958R and Bac 8Fmod-Bac 338Rabc were used throughout this study.
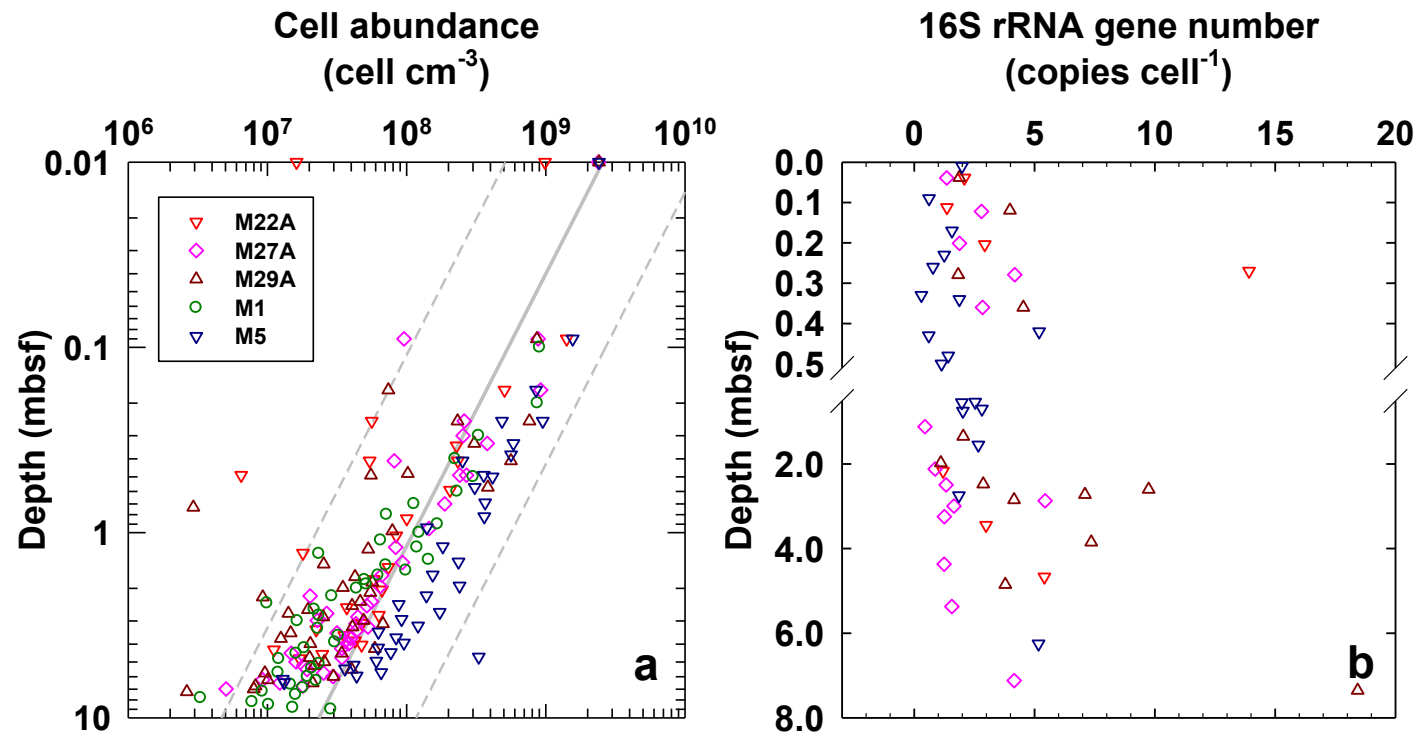
Supplementary Figure 6
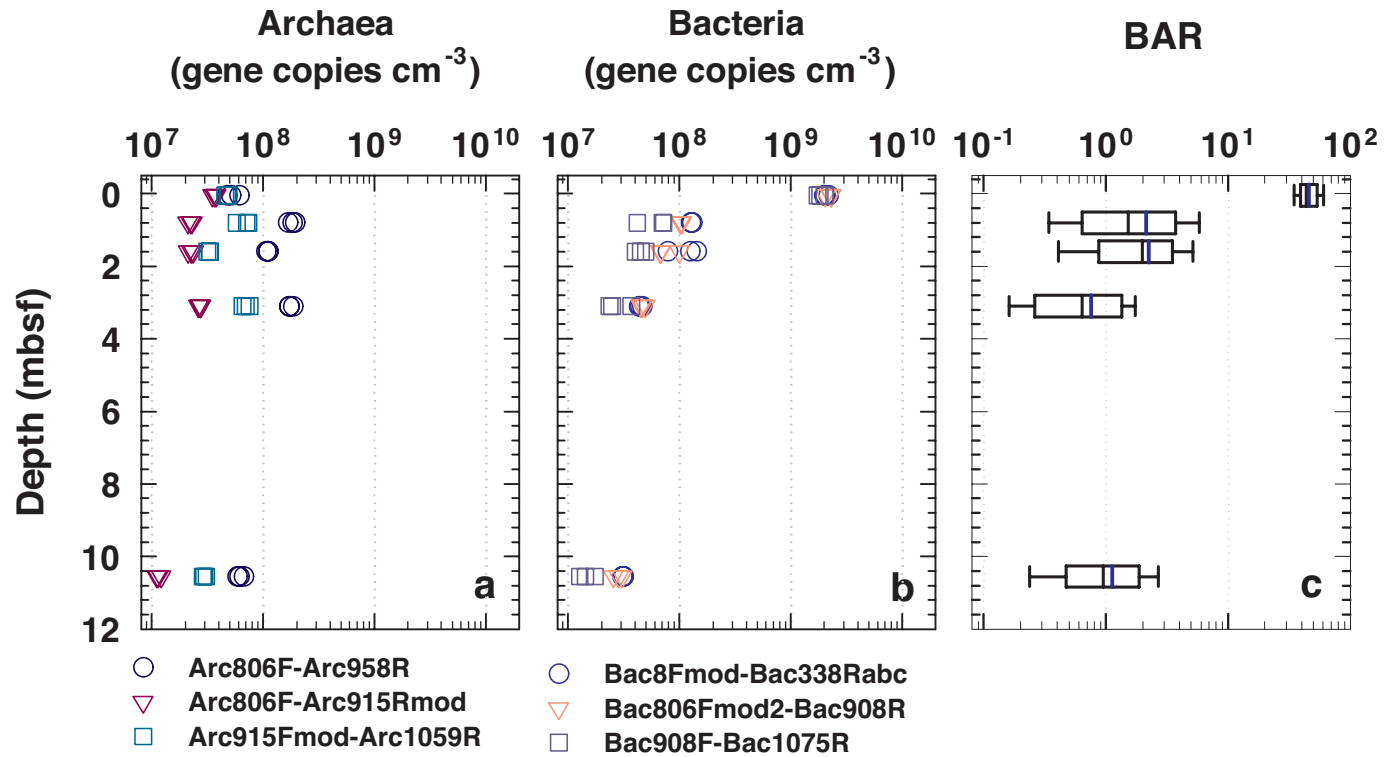
Supplementary Figure 7: Cell abundance profiles at M22A, M27A, M29A, M1, and M5 determined by fluorescence microscopy. The grey dashed line spanning across the lower panels indicates the minimum depth of sediment reworking. The grey shaded areas mark the SMTZ. Data from M1 and M5 were previously published[28]. Note: the SMTZ at M1 was ~0.5m deeper in the M1 core from May 2010 (see below) than in the M1 core from October 2009, which was used for DNA extractions (Supplementary Table 1 and Supplementary Figure 2).

Supplementary Figure 7

Supplementary Figure 8: Cell abundances and 16S gene copy numbers per cell in Aarhus Bay. (a) Depth distribution of cell abundances at M22A, M27A, M29A, M1, and M5 compiled from Supplementary Fig. 7. Cell abundances from M1 and M5 were previously published[28]. The grey solid line is the regression line (Log cell abundance = 8.05 − 0.68 Log depth) and the grey dashed lines indicate the 95% lower and upper prediction limits based on prokaryotic cell abundances in subsurface sediments at 106 locations[29]. **(b)** Depth distributions of 16S gene copy numbers per cell at M22A, M27A, M29A, and M5. The mean copy numbers per cell (averages±standard) at individual stations are: M22A, 4.3±4.2; M27, 2.2±1.4; M29A, 4.2±2.5; M5, 2.0±1.4 copies cell^{-1}. Cell counts and 16S rRNA gene copy numbers were obtained from the same cores (M22A, M27A, M29A), or from parallel cores taken on the same sampling date (M5). We omit data from M1, where cell counts and gene copy numbers were obtained from cores collected on different dates (cell counts: May 2010; DNA: October 2009) and differed clearly in sulfate concentration profiles and the depth of the SMTZ (Supplementary Table 1).

Supplementary Figure 8

Supplementary Figure 9: UPGMA trees (OTU level) for archaeal and bacterial communities among five depths at M1. The UPGMA tree for Archaea was calculated from the archaeal community compositions generated by archaeal primer pairs (A1: Arc806F - Arc958R, A2: Arc806F - Arc915Rmod; A3: Arc915Fmod - Arc1059R). The UPGMA tree for Bacteria was calculated from the bacterial community compositions generated by bacterial primer pairs (B1: Bac8F - Bac338Rabc, B2: Bac806F_mod2 - Bac908R; B3: Bac908F - Bac1075R). Algorithm: Paired group; similarity measurement: Bray-Curtis; number of bootstraps: 1,000. The depths represent the following zones: 5 cmbsf: bioturbation zone, 80 cmbsf: sulfate zone, 160 cmbsf: SMTZ, 310 cmbsf: shallow methane zone, 1055 cmbsf: freshwater peat layer in deep methane zone.

Supplementary Figure 9
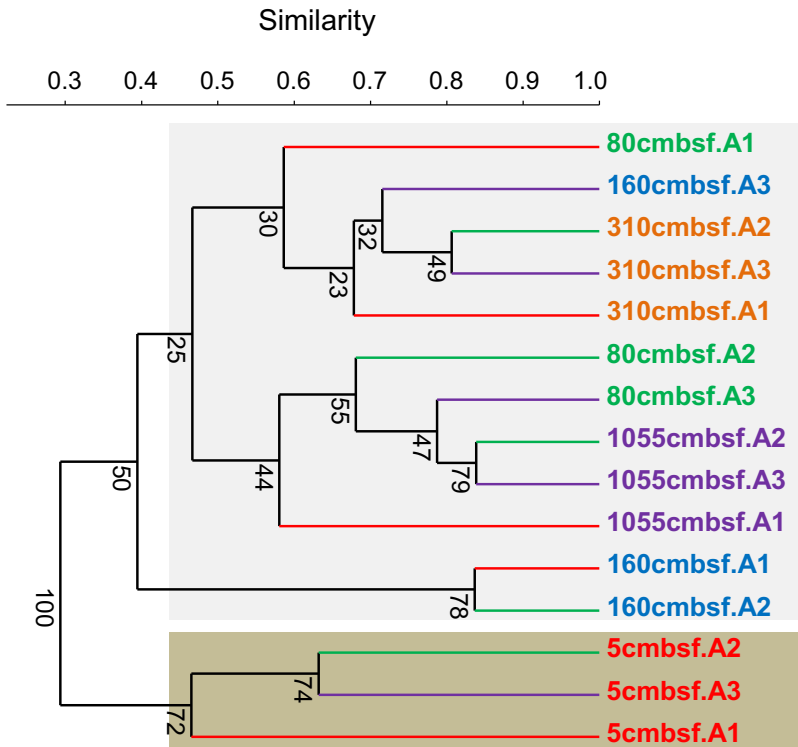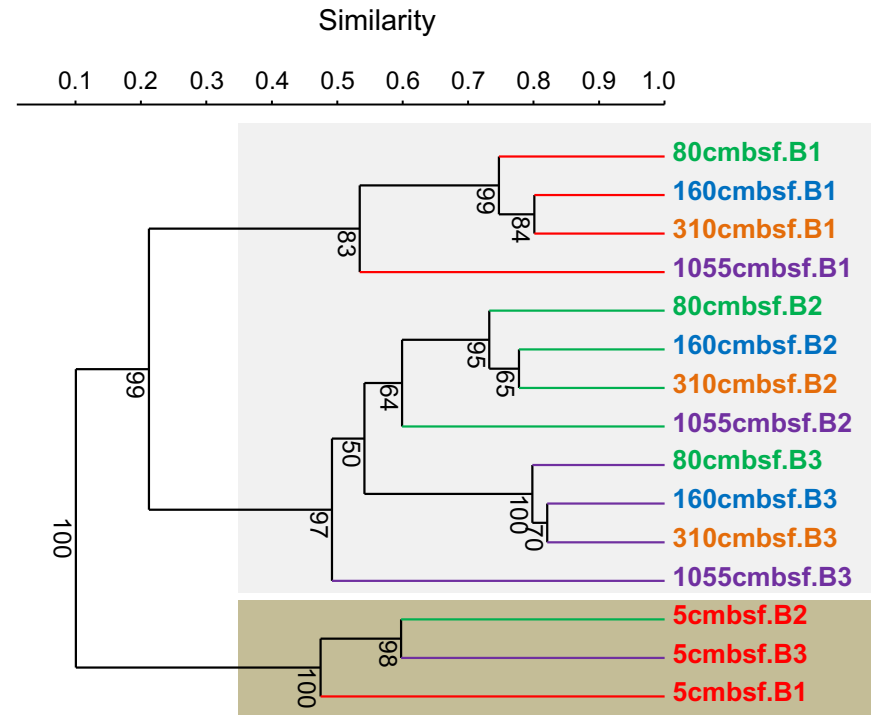
Supplementary References

1.   Holmkvist, L., Ferdelman, T. G. & Jørgensen, B. B. A cryptic sulfur cycle driven by iron in the methane zone of marine sediment (Aarhus Bay, Denmark). *Geochim. Cosmochim. Acta* **75**, 3581-3599 (2011).

2.   Leloup, J.*, et al.* Sulfate-reducing bacteria in marine sediment (Aarhus Bay, Denmark): Abundance and diversity related to geochemical zonation. *Environ. Microbiol.* **11**, 1278-1291 (2009).

3.   Cadillo-Quiroz, H.*, et al.* Vertical profiles of methanogenesis and methanogens in two contrasting acidic peatlands in central New York State, USA. *Environ. Microbiol.* **8**, 1428-1440 (2006).

4.   Yu, Y., Lee, C., Kim, J. & Hwang, S. Group-specific primer and probe sets to detect methanogenic communities using quantitative real-time polymerase chain reaction. *Biotechnol. Bioeng.* **89**, 670-679 (2005).

5.   Nadkarni, M., Martin, F. E., Jacques, N. & Hunter, N. Determination of bacterial load by real-time PCR using a broad-range (universal) probe and primers set. *Microbiology* **148**, 257-266 (2002).

6.   Lever, M. A. , Torti, A., Eickenbusch, P., Michaud, A. B., Šantl-Temkiv, T. & Jørgensen, B. B.A modular method for the extraction of DNA and RNA, and the separation of DNA pools from diverse environmental sample types. *Front. Microbiol.* **6**, (2015).

7.   Ohkuma, M. & Kudo, T. Phylogenetic analysis of the symbiotic intestinal microflora of the termite *Cryptotermes domesticus*. *FEMS Microbiol. Lett.* **164**, 389-395 (1998).

8.   Schloss, P. D.*, et al.* Introducing mothur: open-source, platform-independent, community-supported software for describing and comparing microbial communities. *Appl. Environ. Microbiol.* **75**, 7537-7541 (2009).

9.   Bragg, L., Stone, G., Imelfort, M., Hugenholtz, P. & Tyson, G. W. Fast, accurate error-correction of amplicon pyrosequences using Acacia. *Nature Meth.* **9**, 425-426 (2012).

10.   Edgar, R. C., Haas, B. J., Clemente, J. C., Quince, C. & Knight, R. UCHIME improves sensitivity and speed of chimera detection. *Bioinformatics* **27**, 2194-2200 (2011).

11.   Hammer, Ø., Harper, D. A. T. & Ryan, P. D. Paleontological statistics software package for education and data analysis. *Palaeontol. Electron.* **4**, 9-18 (2001).

12.   Maire, O., Duchene, J. C., Rosenberg, R., de Mendonca Jr., J.B. & Gremare, A. Effects of food availability on sediment reworking in *Abra ovata* and *A. nitida*. *Mar. Ecol. Prog. Ser.* **319**, 135-153 (2006).

13.   Thayer, C. W. Sediment-mediated biological disturbance and the evolution of marine benthos. In: *Biotic Interactions in Recent and Fossil Benthic Communities* (eds Tevesz MJS). Plenum Press (1983).

14.   Dauwe, B., Herman, P. M. J. & Heip, C. H. R. Community structure and bioturbation potential of macrofauna at four North Sea stations with contrasting food supply. *Mar. Ecol. Prog. Ser.* **173**, 67-83 (1998).

15.   Fallesen, G. *The ecology of macrozoobenthos in Aarhus Bay, Denmark* PhD thesis, University of Stirling, (1994).

16.   Josefson, A. B. & Rosenberg, R. Long-term soft-bottom faunal changes in three shallow fjords, West Sweden. *Neth. J. Sea. Res.* **22**, 149-159 (1988).

17.   O'Foighil, D., McGrath, D., Conneely, M. E., Keegan, B. F. & Costelloe, M. Population dynamics and reproduction of *Mysella bidentata* (Bivalvia: Galeommatacea) in Galway Bay, Irish west coast. *Mar. Biol.* **81**, 283-291 (1984).

18.   Kiørboe, T. & Møhlenberg, F. Particle selection in suspension-seeding bivalves. *Mar. Ecol. Prog. Ser.* **5**, 291-296 (1981).

19.   Yonge, C. M. On the habits and adaptations of *Aloidis* (*Corbula*) *gibba*. *J. Mar. Biol. Assoc. U.K.* **26**, 358-376 (1946).

20.   Richman, S. E. & Lovvorn, J. R. Effects of clam species dominance on nutrient and energy acquisition by spectacled eiders in the Bering Sea. *Mar. Ecol. Prog. Ser.* **261**, 283-297 (2003).

21.   Gogina, M. & Zettler, M. L. Diversity and distribution of benthic macrofauna in the Baltic Sea. *J. Sea Res.* **64**, 313-321 (2010).

22.   Clark, R. B. Observations on the food of *Nephtys*. *Limnol. Oceanogr.* **7**, 380-385 (1962).

23.   Michaud, E., Aller, R. C. & Stora, G. Sedimentary organic matter distributions, burrowing activity, and biogeochemical cycling: Natural patterns and experimental artifacts. *Estuar. Coast. Shelf Sci.* **90**, 21-34 (2010).

24.   Pedersen, T. F. & Munkegade, N. Metabolic adaptations to hypoxia of two species of Polychaeta, *Nephtys ciliata* and *Nephtys hombergii. Mar. Biol.* **161**, 213-215 (1991).

25.   Dobbs, F. & Scholly, T. Sediment processing and selective feeding by *Pectinaria koreni* (Polychaeta: Pectinariidae) *Mar. Ecol. Prog. Ser.* **29**, 165-176 (1986).

26.   Buchanan, J. B. The biology of *Echinocardium cordatum* [Echinodermata: Spatangoidea] from different habitats. *J. Mar. Biol. Assoc. U.K.* **46**, 97-114 (1966).

27.   Jensen, J. B. & Bennike, O. Geological setting as background for methane distribution in Holocene mud deposits, Aarhus Bay, Denmark. *Cont. Shelf Res.* **29**, 775-784 (2009).

28.   Langerhuus, A. T.*, et al.* Endospore abundance and d:l-amino acid modeling of bacterial turnover in holocene marine sediment (Aarhus Bay). *Geochim. Cosmochim. Acta* **99**, 87-99 (2012).

29.   Parkes, R. J.*, et al.* A review of prokaryotic populations and processes in sub-seafloor sediments, including biosphere: Geosphere interactions. *Mar. Geol.* **352**, 409-425 (2014).